

# **Optical Detection of Immunoglobulin E**

By

Saadia Ranginwala  
B.S., Minnesota State University, 2008

THESIS

Submitted as partial fulfillment of the requirements  
for the degree of Master of Science in Bioengineering  
in the Graduate College of the  
University of Illinois at Chicago, 2012

Chicago, Illinois

Defense Committee:

Michael Stroschio, Chair and Advisor  
Michael Cho  
Mitra Dutta, Electrical and Computer Engineering

## **AKNOWLEDGEMENTS**

I would like to thank my thesis advisor, Dr. Stroschio, for all of his help and support throughout my project. I sincerely appreciate, how he helped me come up with a good project, and all of his advice on how to approach the project. I also appreciate the experience I gained in his lab. I would also like to thank my other two thesis committee members, Dr. Michael Cho, and Dr. Mitra Dutta for being on my committee.

**SR**

## TABLE OF CONTENTS

<u>CHAPTER</u>	<u>PAGE</u>
<b>1. INTRODUCTION.....</b>	<b>Error! Bookmark not defined</b>
1.1. Aptamers.....	<b>Error! Bookmark not defined</b>
1.2. The Process of Selecting Aptamers (SELEX).....	1
1.3. The Advantages of Aptamers over Antibodies .....	2
1.4. Immunoglobulin E and its Significance .....	3
<b>2. EXPERIMENTAL THEORY.....</b>	<b>4</b>
2.1. Quantum Dots.....	4
2.2. Fluorescence Resonant Energy Transfer and Quenchers .....	5
<b>3. EXPERIMENTAL DESIGN.....</b>	<b>5</b>
3.1. Immunoglobulin E Aptamer Sequence .....	5
3.2. Gibbs Free Energy Prediction .....	6
3.3. Discussion .....	11
3.4. Proposed Design of Immunoglobulin E Optical Sensor.....	11
<b>4. RAMAN SPECTROSCOPY .....</b>	<b>12</b>
4.1. Raman and Surface Enhanced Raman Spectroscopy (SERS).....	12
4.2. Cancer Detection and Raman Spectroscopy.....	17
4.3. Methods and Materials .....	18
4.4. Results .....	18
4.5. Discussion and Conclusion.....	27
<b>CITED LITERATURE.....</b>	<b>27</b>
<b>BIBLIOGRAPHY .....</b>	<b>29</b>
<b>VITA.....</b>	<b>30</b>

## LIST OF TABLES

<u>TABLE</u>		<u>PAGE</u>
1.	Tabulated results of SERS spectra of 0.1 $\mu\text{M}$ solution .....	20
2.	Tabulated results SERS spectra of 1.0 $\mu\text{M}$ solution .....	22
3.	Tabulated results of SERS spectra of 2.0 $\mu\text{M}$ solution.....	24
4.	Tabulated results of SERS spectra of 5.0 $\mu\text{M}$ solution.....	26

## LIST OF FIGURES

<u>FIGURE</u>		<u>PAGE</u>
1.	First folding prediction of 81 base pair sequence .....	7
2.	Second folding prediction of 81 base pair sequence.....	8
3.	First folding prediction of IgE aptamer sequence.....	9
4.	Second folding prediction of IgE aptamer sequence .....	10
5.	Raman Spectroscopy schematic.....	15
6.	Graphical representation of SERS Spectra of 0.1 $\mu\text{M}$ solution .....	19
7.	Graphical representation of SERS Spectra of 1.0 $\mu\text{M}$ solution .....	21
8.	Graphical representation of SERS Spectra of 2.0 $\mu\text{M}$ solution .....	23
9.	Graphical representation of SERS Spectra of 5.0 $\mu\text{M}$ solution .....	25

## **LIST OF ABBREVIATIONS**

SELEX Systematic Evolution of Ligands by Exponential Enrichment

IgE Immunoglobulin E

FRET Fluroescent Resonant Energy Transfer

SERS Substrate Enhanced Raman Spectroscopy

## **SUMMARY**

Aptamers have a wide range of applications in clinical applications. A review of aptamers, and their applications has been given. Immunoglobulin E is an antibody associated with allergic reactions, and immune deficiency related diseases. The aptamer for Immunoglobulin E was found in the literature. An optical sensor, for the detection of Immunoglobulin E, was designed. The aptamer for Immunoglobulin was the main part of the designed sensor. Raman spectroscopy provides the molecular fingerprint of biological molecules. Substrate Enhanced Raman Spectroscopy was performed in order to obtain a molecular fingerprint of the Immunoglobulin E aptamer.

# 1. INTRODUCTION

## **1.1. Aptamers**

Nucleic Acids have the ability to hybridize to one another, and nucleic acids also have the ability to form complex shapes. The complex shapes can act as scaffolds for molecular interactions. The complex shapes can also provide the support for formation of complexes with protein and small molecule targets. Biological nucleic acids, meaning, nucleic acids which exist naturally, have these abilities. Recent technological advances have made it possible to produce non-biological oligonucleotides that can bind to specific protein targets [1].

Aptamers are DNA or RNA sequences, that are selected in vitro, based on their ability to bind to specific protein targets [2]. Aptamers are short, single stranded DNA or RNA molecules, which usually have a length between 15 to 100 nucleotides. Aptamers bind to specific protein targets via non-covalent interactions [3]. Aptamers have the ability to become unique tertiary structures, which helps in the selective binding to the respective protein target [4].

Aptamers have the ability to be produced for a specific function, and aptamers also have impressive selectivity and sensitivity. This is why aptamers are commonly used as recognition elements for biosensor applications, and have been used in a multitude of sensing technologies [2].

## **1.2. The Process of Selecting Aptamers (SELEX)**

Recent technology in DNA synthesis allows for degenerate deoxynucleotides to be produced in large populations. Polymerase Chain Reaction (PCR) allows a small number of molecules to be amplified to an amount that can be manipulated by researchers. The production

of a large population of random DNA sequences, the ability to do PCR on the relevant sequences, and the ability to separate the specific oligonucleotides based on their binding or catalytic activities, gave rise to the process of Systematic Evolution of Ligands by Exponential Enrichment (SELEX) [1].

The process of SELEX is started by a DNA or RNA library, consisting of  $10^{14}$  -  $10^{15}$  different sequences. The library consists of 20-60 nucleotide long random regions, which are flanked by defined constant 5' and 3' regions. The fixed region consists of a promoter region for T7 RNA polymerase, and primers for reverse transcription and polymerase chain reaction [5].

The double stranded oligonucleotide library is converted to single stranded DNA, during DNA SELEX, and is then transcribed to RNA by in vitro transcription, during RNA SELEX. In the process of RNA SELEX, the random RNA molecules adapt secondary structures, and are then incubated with target molecules. The aptamers that bind to the targets are selected from the aptamers that don't bind to the targets. The target-bound aptamers are then reverse-transcribed and PCR amplified. This provides a new DNA library, and a new round of selections begin. This process is repeated, and aptamers with increasing affinity and specificity are obtained. The process is repeated until the DNA pool is saturated with dominating aptamers [5].

### **1.3. The Advantages of Aptamers Over Antibodies**

Antibodies exist naturally in the body, and their purpose is to target foreign pathogenic proteins, in order to neutralize and destruct the proteins. The antibodies function by the expressing a set of variable amino acids on the tips of the antibody, and the tips, which are called paratopes, bind to the foreign proteins. The paratopes interact with the foreign proteins through non-covalent hydrogen and ionic bonds, and hydrophobic, and van der Waals interactions.

There are twenty different amino acids in the human body that are used to create a diversity of paratopes that bind to antigens [3].

Antibodies are useful for many bioanalytical applications, but some shortcomings involved with using antibodies are that they are large, immunogenic, and hard to functionalize. Some other disadvantages of using antibodies are that they have little tissue penetration, have variability between batches, and they also need careful storage [3].

There are several advantages of using aptamers over antibodies. With aptamers, it is possible to target any molecule, so there is no limitation with the requirement of using cell lines or animals as it is required when using antibodies. Aptamers can also be produced with high purity, as it's possible to produce a large quantity of aptamers via subsequent cycles of polymerase chain reaction. Aptamers can be easily altered by modifications with functional groups, in order to serve different purposes. Aptamers are also more stable than antibodies, so the aptamers are able to survive harsh conditions, such as high temperature or extreme pH [6].

#### **1.4. Immunoglobulin E and its Significance**

Immunoglobulin E plays a role in allergic asthmatic disease, by way of attaching to the IgE receptors, and thus triggering a series of cellular events. The series of cellular events triggers many factors that play an integral part in the potential of disease symptoms. There have been studies in the mouse, and they indicate that if IgE levels were reduced, then the allergic inflammatory response, associated with diseases such as asthma, would be attenuated. Therefore, IgE is a good target for new therapeutic agents. IgE also has a significant role in other allergic conditions such as allergic rhinitis and allergies to various substances [7].

IgE has been known in mediating hypersensitivity. When compared to other antibodies in human serum, IgE is the least abundant. Concentration of human Immunoglobulin G is usually in the concentration of 10 mg/mL, and the concentration of Immunoglobulin E rarely exceeds 10 ng/mL [7].

## **2. EXPERIMENTAL THEORY**

### **2.1. Quantum Dots**

Quantum Dots are semiconductor crystals, at the nanoscale size. When a photon of light hits a semiconductor at the nanoscale, some of the electrons are excited into higher energy states, and then they release a photon of a frequency specific to the material, when returned to the ground state. Semiconductor and metal particles which are in the size range of 2-6 nm have similarities with biological molecules such as nucleic acids, and proteins, so they are of great interest [8].

Quantum dots have many advantages over currently used fluorophores, such as organic dyes, and fluorescent proteins. Quantum dots can be excited by a wide range of wavelengths, so they can be manipulated to simultaneously excite different colored quantum dots, with only a single wavelength. Quantum dots also have narrow emission spectra, and can be easily controlled by varying the core size and composition, and by varying the surface coatings. Quantum dots can be manipulated to emit light at different precise wavelengths, ranging from ultraviolet to infrared. The properties that make them good for multiple simultaneous imaging, are their narrow emission and broad absorption spectra, and they can be used to encode genes, proteins, and small-molecule libraries [8].

## **2.2 Fluorescent Resonant Energy Transfer (FRET) and Quenchers**

Fluorescent Resonance Energy Transfer (FRET) is the transfer of energy from a donor molecule to an acceptor, and it is dependent on distance. FRET is sensitive to distance, and it is used to study molecular interaction. The donor molecule can be a dye or chromophore, which is the initial absorber of energy, and the acceptor is the chromophore to which the energy is transferred. The resonance happens over a greater distance than an interatomic distance, and there is no conversion to thermal energy, as the transfer of energy results in the reduction of fluorescence in the donor molecule, and an increase in the acceptor's emission intensity. In order for FRET to occur, the donor and acceptor molecules must be close to each other, usually between 10 to 100 Angstrom. The acceptor and donor must have overlapping excitation spectrum and fluorescence emission spectrum [9].

A dark quencher is a chromophore that can absorb a photon and be excited to a higher electronic state. Dark quenchers can relax to the ground state without giving off radiation. Dark quenchers can be used at high concentrations, because they don't have significant intrinsic fluorescence. Quantum dots can be used in combination with a quencher, and FRET would occur [10].

## **3. EXPERIMENTAL DESIGN**

### **3.1. Immunoglobulin E Aptamer Sequence**

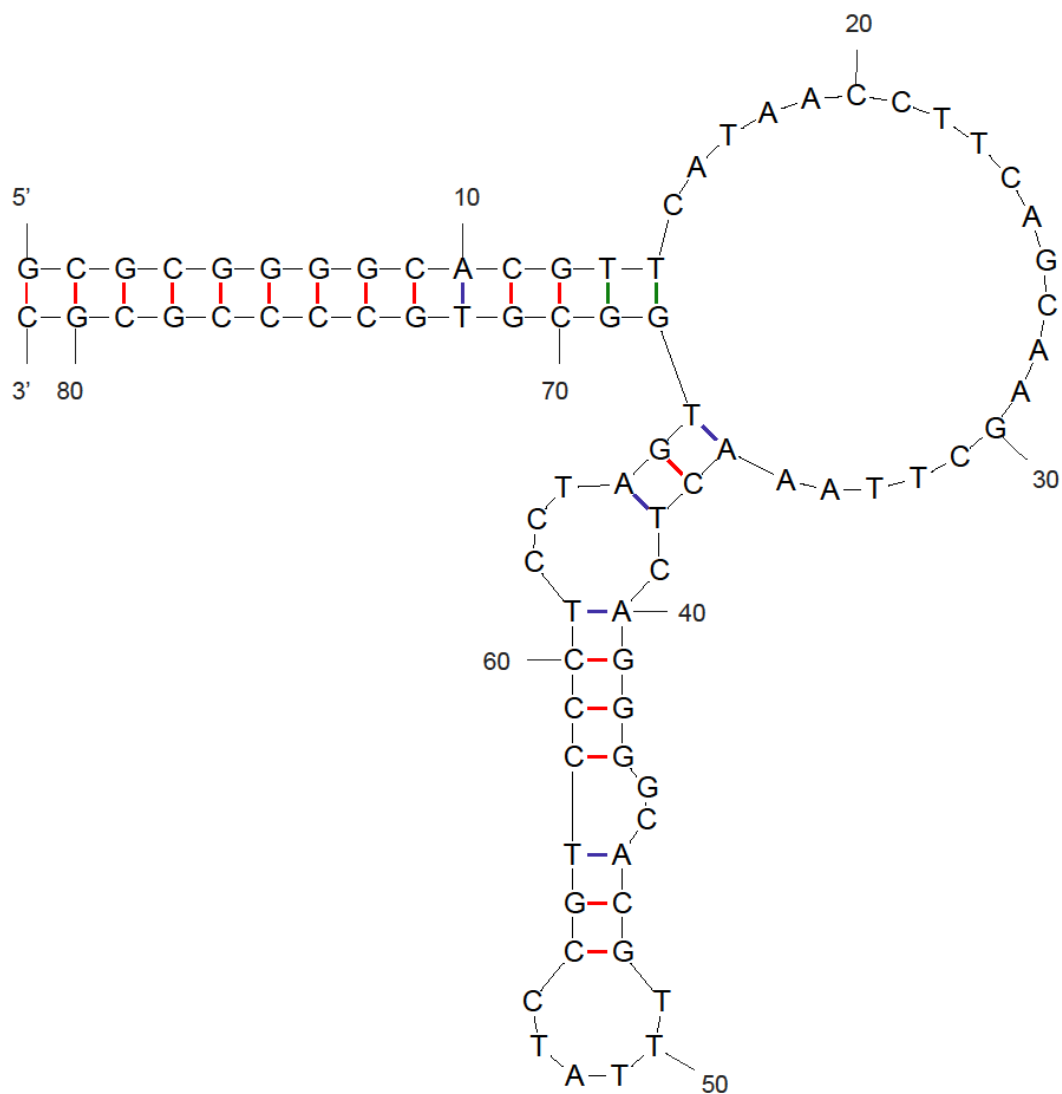
The aptamer for Immunoglobulin E was found in the literature, specifically by a paper by Wu et al. In the study, the researchers prepared an 81 base pair sequence, that contained the 37 base pair aptamer sequence, and spacer sequences. The sequence of the 81 base pair sequence is 5'-HS-(CH<sub>2</sub>)<sub>6</sub>-GCGCG GGGCA CGTTCA TAACC TTCAG CAAGC TAAA CTCAG GGGCA CGTTT ATCCG TCCCT CCTAG TGGCG TGCCC CGCGC-3'. The underlined

parts are complementary to each other, and the bold base pairs are part of the actual aptamer sequence [11].

### **3.2 Gibbs Free Energy Prediction**

Gibbs Free Energy is the energy that is available to do work within a system. Free energy is the source of energy needed for things, such as a chemical reaction, to happen. The Gibbs free energy or  $\Delta G$  is the difference between the  $G$  of the reactants and the  $G$  of the products. The Gibbs Free Energy is the maximum potential energy of a system that can be used. If the  $\Delta G$  is negative, then the reaction is thermodynamically favorable, because the products are at a lower energy than the reactants, and according to the second law of thermodynamics, a reaction will always want to proceed toward a lower energy state. So the lower the Gibbs Free energy, the more likely it is for a reaction to occur [12].

A DNA folding software website called MFold was used to predict the Gibbs Free Energy for the aptamer sequences [13]. The website has a software where you can input the sequence, and it will generate predictions on how the DNA will fold, and the corresponding free energies. The units of the Gibbs Free energy is in kcal/mol. Figures were generated for the full 81 base pair sequence mentioned in the literature, and the sequence of the aptamer itself.



$dG = -17.93$  12Aug22-15-32-59

Figure 1. The first folding prediction of the 81 base pair sequence which has the aptamer sequence, and the other spacer sequences. The Gibbs Free Energy is  $-17.93$  kcal/mol [13].

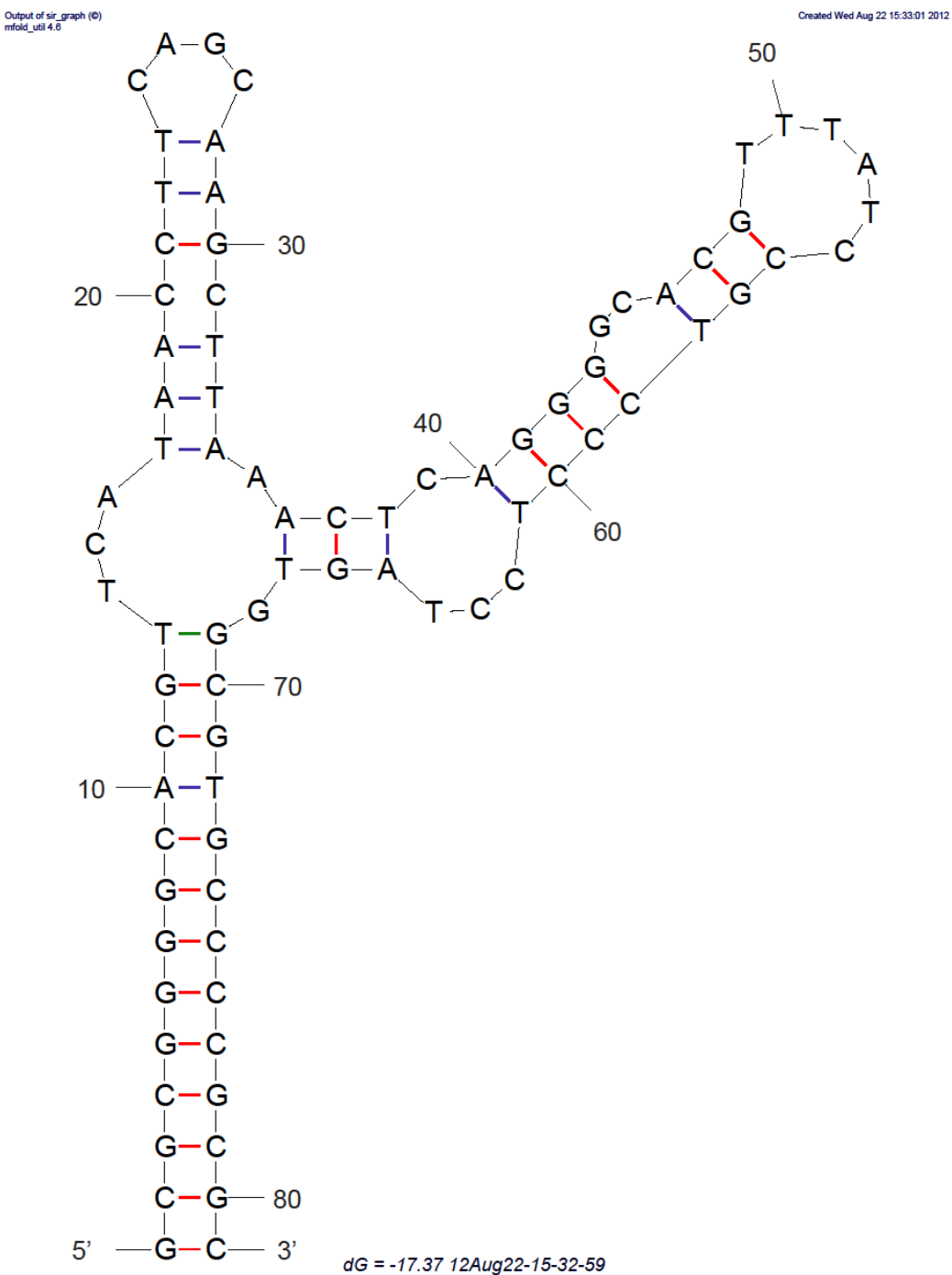


Figure 2. The second folding prediction of the 81 base pair sequence which has the aptamer sequence, and the other spacer sequences. The Gibbs Free Energy is  $-17.37$  kcal/mol [13].





### **3.3. Discussion**

Figures 1 and 2 illustrate the sequences that Wu et al. used for their study. The Gibbs Free Energy shows that the DNA is going to favor folding in that way, as the Gibbs Free Energy is more negative than the energy of the aptamer itself. However, the structure is quite complicated, with many loops, and it will be difficult to create a sensor out of something so bulky.

The aptamer sequence, which is illustrated in Figures 3 and 4, is smaller, and also forms a hairpin structure. Figure 3 shows the Gibbs Free Energy being lower, and is also more favorable for creating an optical sensor. The hairpin structure is formed, because the base pairs are complementary to each other.

### **3.4. Proposed Design of Immunoglobulin E Optical Sensor**

The most practical sequence to use is the aptamer sequence alone. The two folding predictions for this aptamer are illustrated in figures 3 and 4. The more likely configuration will be figure 3, as the Gibbs Free Energy is lower. However, the energy difference between the two configurations is not very significant, so it is likely that the aptamer will fold in the configuration of figure 4 almost as much as the aptamer will fold in the configuration of figure 3. Both configurations will be compatible with the design of the Immunoglobulin E optical sensor.

As explained earlier, quantum dots are good for using with biological macromolecules such as DNA. Using the concept of Fluorescence Resonant Energy Transfer, a quantum dot can be used in conjunction with a dark quencher, in order to detect Immunoglobulin E.

The quantum dot can be modified with carboxyl groups, and either the 5' end or 3' end can be modified with amine groups, so that the quantum dot will attach to the modified side.

When purchasing the aptamer from Integrated DNA Technologies, the DNA can be ordered to have the other end to be modified with a dark quencher.

In the absence of Immunoglobulin E, the aptamer will be in the hairpin structure, illustrated in Figure 3, and the fluorescence from the quantum dot will be quenched from the dark quencher, since they will be in the FRET distance. Once the aptamer is put into a solution with Immunoglobulin E, the binding between the aptamer and Immunoglobulin E should theoretically overcome the binding energy between the complementary base pairs in the aptamer. The IgE will cause the hairpin sequence to open, due to binding to the aptamer, and the quantum dot and quencher will no longer be within FRET distance. Therefore, the quantum dot will start fluorescing, and this will be a signal for the presence of Immunoglobulin E.

#### **4. RAMAN SPECTROSCOPY**

##### **4.1 Raman and Surface Enhanced Raman Spectroscopy (SERS)**

Raman spectroscopy is the phenomena of inelastic scattering of light, which was discovered in 1928 by Chandrashekhara Venkata. The inelastic scattering of light is known as the Raman effect. The Raman effect is what happens when the frequency of radiation of the incident beam is different from the frequency of the radiation of the scattered molecules, and there is a shift in wavelength. The chemical structure, of the molecules that cause the scattering, is what the shift in wavelength depends on [14]. The scattered light is used to gain information about the molecular vibrations, which can provide information about the structure, symmetry, electronic environment, and bonding of the molecule. This allows for quantitatively and qualitatively analyzing individual compounds [14].

Raman spectroscopy is a spectroscopic technique which is used in studying biological materials, such as proteins, DNA, and chromosomes. The technique of Raman spectroscopy

gives information about the chemical composition, the secondary structure, and the chemical surrounding of specific subunits, of the material being studied [15].

Raman spectroscopy uses a non-ionizing laser, as the excitation source. The material being studied can absorb, scatter, or have the incident photons pass through it with no interaction. If the energy gap between the ground state and excited state of a molecule matches the energy of the incident photon, then most likely, the photon will be absorbed by the molecule, and the molecule will be promoted to the excited state. When the excited molecule relaxes to the ground state by emission of a photon, fluorescence occurs. When the incident photon distorts the electron clouds of the material, scattering occur [16].

In visible light, the two scattering types that occur are Rayleigh and Raman scattering. Rayleigh scattering is the more intense form of scattering, and it happens when the electron clouds are distorted. Since there is no energy exchange occurring, this is an elastic process. When the vibrational state of the molecule is changed, there is a transfer of energy, either from the photon to the molecule, or from the molecule to the photon. Raman scattering is inelastic, because of the energy transfer occurring, however, it is a weak process that involves about one in every  $10^6$  to  $10^8$  scattered photons [16].

As mentioned above, the energy exchange can be from the molecule to the photon, or from the photon to the molecule. Due to there being two different directions of energy transfer, Raman scattering is categorized into Stokes and anti-Stokes. Stokes scattering is when the molecule absorbs energy from the incident photon and is elevated from a lower energy state to an excited vibrational state. Anti-Stokes scattering occurs when a molecule may have been previously in an excited state, before the interaction between the incident photon and the molecule, so the molecule releases energy after interacting with the incident photon, and returns

to a lower energy state. Therefore, the photons that are scattered in an anti-Stokes process are higher in energy than the incident photons [16].

Stokes scattering is usually the dominant scattering process, because molecules are usually in the ground state at room temperature, so the scattering commonly recorded for Raman spectroscopy is Stokes scattering. The energy difference between the incident photons and scattered photons is called a Raman band shift, and the Raman band shift is usually described in wavenumber, and the unit that is commonly used to indicate wavenumber is  $\text{cm}^{-1}$ . The wavenumber in  $\text{cm}^{-1}$  can be converted to Joules, via a conversion factor  $hc$ , where  $h$  is Planck's constant, and  $c$  is the speed of light [16].

A Raman spectroscopy system is typically set up with an incident laser, which irradiates the sample by an optical microscope, and the Raman scattered photons are collected into a spectrometer, which is appropriately filtered. The lasers which are used can be of different wavelengths, such as a HeNe laser has a wavelength of 533 nm, and a Ti:sapphire laser can be tuned from 650 nm to 1100 nm. With biological samples, longer wavelengths are typically used, because longer wavelength excitations result in less fluorescence background [16]. Figure 5 illustrates the typical setup of a Raman Spectroscopy system.

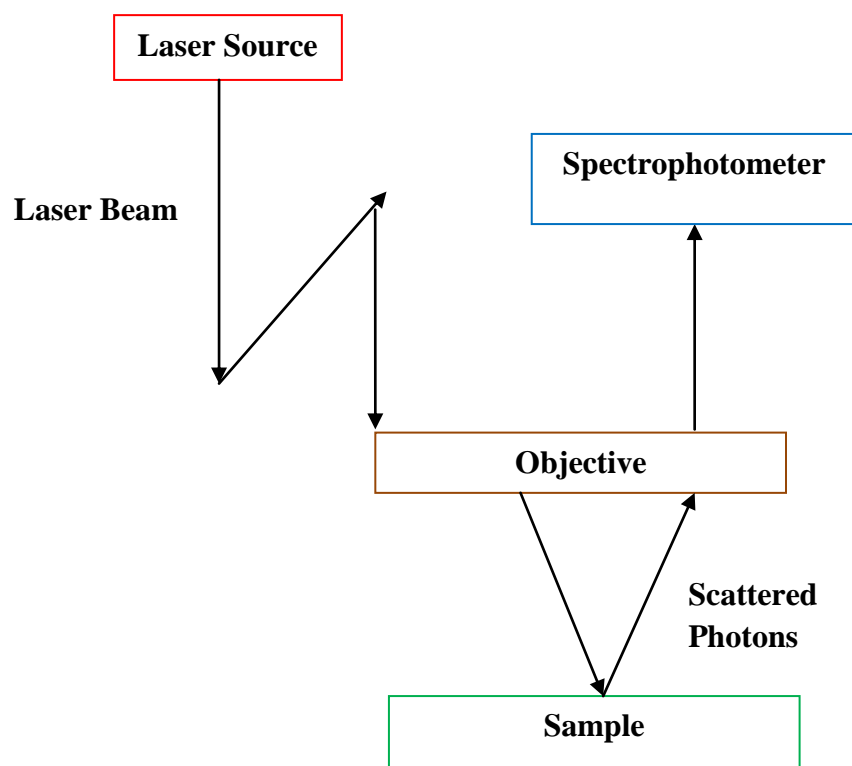


Figure. 5. Laboratory setup of a Raman Spectroscopy System.

A disadvantage of the Raman spectroscopy technique, is that there is generally a small scattering cross-section for biological molecules, so high concentrations of the sample must be used. However, biological compounds of interest are not easy to prepare in large amounts, so the compounds cannot be studied using normal Raman spectroscopy, added to that is the fact that a laser with a high power, of about 300 mW would be needed [15].

It is well known, that when molecules are adsorbed on metal surfaces, or metal particles in solution, the Raman scattering is enhanced, and this enhancement also occurs for large and complicated molecules. The phenomenon of this enhanced scattering is called Surface Enhanced Raman Scattering (SERS) [15]. Through SERS, the Raman signal level is enhanced, because the interaction between the molecule and the nanoscale metal surface is exploited. Raman signals can be enhanced by a factor in the range of  $10^3 - 10^{14}$ , depending on the definition of the

enhancement factor [16]. The most common definition used for the average SERS enhancement factor is

$$EF = \{ I_{\text{SERS}} / N_{\text{SURF}} \} / \{ I_{\text{RS}} / N_{\text{VOL}} \}$$

where  $I_{\text{SERS}}$  is the SERS intensity,  $I_{\text{RS}}$  is the regular Raman intensity,  $N_{\text{VOL}}$  is the average number of molecules in the scattering volume for regular Raman, and  $N_{\text{SURF}}$  is the average number of molecules in the scattering volume for SERS [16].

There have been many theories that have been developed to explain why there is such a large enhancement factor due to SERS. Since such a large enhancement factor exists, a combination of enhancement mechanisms is needed to explain the large enhancement factor. Two mechanisms have been proposed to explain the enhancement factor [15]. One of the mechanisms is of the enhanced field strength. Near the roughened surfaces, there is an increased field strength because of the resonant excitation of collective oscillations in metals that are free-electron-like, such as Ag, Au, and Cu, due to the incident laser field. The enhancement factor from this mechanism is in the range of  $10^3$  to  $10^5$ . The other mechanism used to explain the enhancement factor is of the presence of an active site. This mechanism theorizes that there is a presence of structures on the surface which are capable of forming certain molecular configurations. Experimental evidence proves that this plays a role in the enhancement as there is an irreversible loss in the intensity when the potential of the electrode is lowered, or the temperatures is increased to the point where the structures are destroyed. The enhancement due to the active site is limited to the molecular sp layer which is in direct contact with the metal surface, and there is either a physical or chemical bonding between the molecule that is adsorbed, and the surface [15].

## **4.2 Cancer Detection and Raman Spectroscopy**

Since cancer is the second most common cause of death in the United States, effective cancer treatments rely on early detection and the accurate diagnosis of a cancer. There have been various reports of Raman spectroscopic studies on cancers, and Tu et al. have reviewed the use of Raman spectroscopy on breast cancer, colorectal cancer, and cervical cancer, which are the three most commonly seen carcinomas [16].

There have been many studies in which Raman spectroscopy was used in the detection of precancerous and cancerous breast tissues. According to studies done by Haka and colleagues, which were some of the studies Tu et al. reviewed, Raman spectroscopy had the ability to distinguish between normal, benign, and malignant lesions of breast ex vivo, with a sensitivity of 94 % and a specificity of 96 % [16].

In cervical cancer, while using Raman spectroscopy, algorithms to differentiate between diseased and normal cervical tissue were designed, and Robichaux-Viehoever et al. were able to get results of 89% sensitivity, and 81% specificity. Kater and colleagues used different algorithms, and they were able to achieve a sensitivity of 98 % and a specificity of 96 %. The most commonly used screening method for cervical cancer, Papanicolaou (Pap) smear has a detection specificity of 96.8% and a sensitivity of 55.4% [16].

For colorectal cancer, several different methods have been developed, and have been effective in the detection of colorectal cancer. Widjaja and colleagues have been able to differentiate between different types of pathological colonic tissues, including normal tissue, polyps, and cancer, with a sensitivity and specificity greater than 98 %. Beljebbar et al generated pseudo-color maps of normal and cancerous tissues by using Raman spectra of individual tissue constituents, including proteins, lipids, collagen, nucleic acid, and mucus. The use of the maps

showed that proteins can be used as potential spectroscopic biomarkers for the differentiation of adenocarcinomatous tissues [16].

### **4.3 Methods and Materials**

The IgE aptamer was ordered from a company known as Integrated DNA Technologies. The aptamer was received in powder form, and was then dissolved in deionized water to make concentrations of 0.1 micromolar ( $\mu\text{M}$ ), 1  $\mu\text{M}$ , 2  $\mu\text{M}$ , and 5  $\mu\text{M}$ . Twenty microliters of each of the aptamer, in solution form, were applied to a different well in the SERS substrate. The samples were then dried overnight, and were then rinsed with deionized water after being dried for twenty four hours, and the samples were then air dried/tissue dried for a couple of minutes. The SERS substrate with the loaded samples was then taken to do SERS.

The Raman imaging system was started, and the laser was set to 1 % transmission, at a power of 23.5 mW. Each sample was imaged for thirty seconds, at the previous mentioned power and laser transmission.

The substrate used to perform Surface Enhanced Raman spectroscopy was received from a student at the University of Georgia Athens. The Ag nanorod substrate was fabricated by oblique angle deposition. The SERS substrate was designed in a way that the wells in the substrate were equally spaced, and were isolated from each other so there is no cross-contamination [17].

### **4.4 Results**

The experimental peaks from the SERS performed above were compared to previously identified peaks in the literature, specifically from a well known journal article by C. Otto et al. [18]. The journal article has identified many peaks using SERS, and has compared the SERS peaks with normal Raman peaks. The following several graphs illustrate the results obtained.

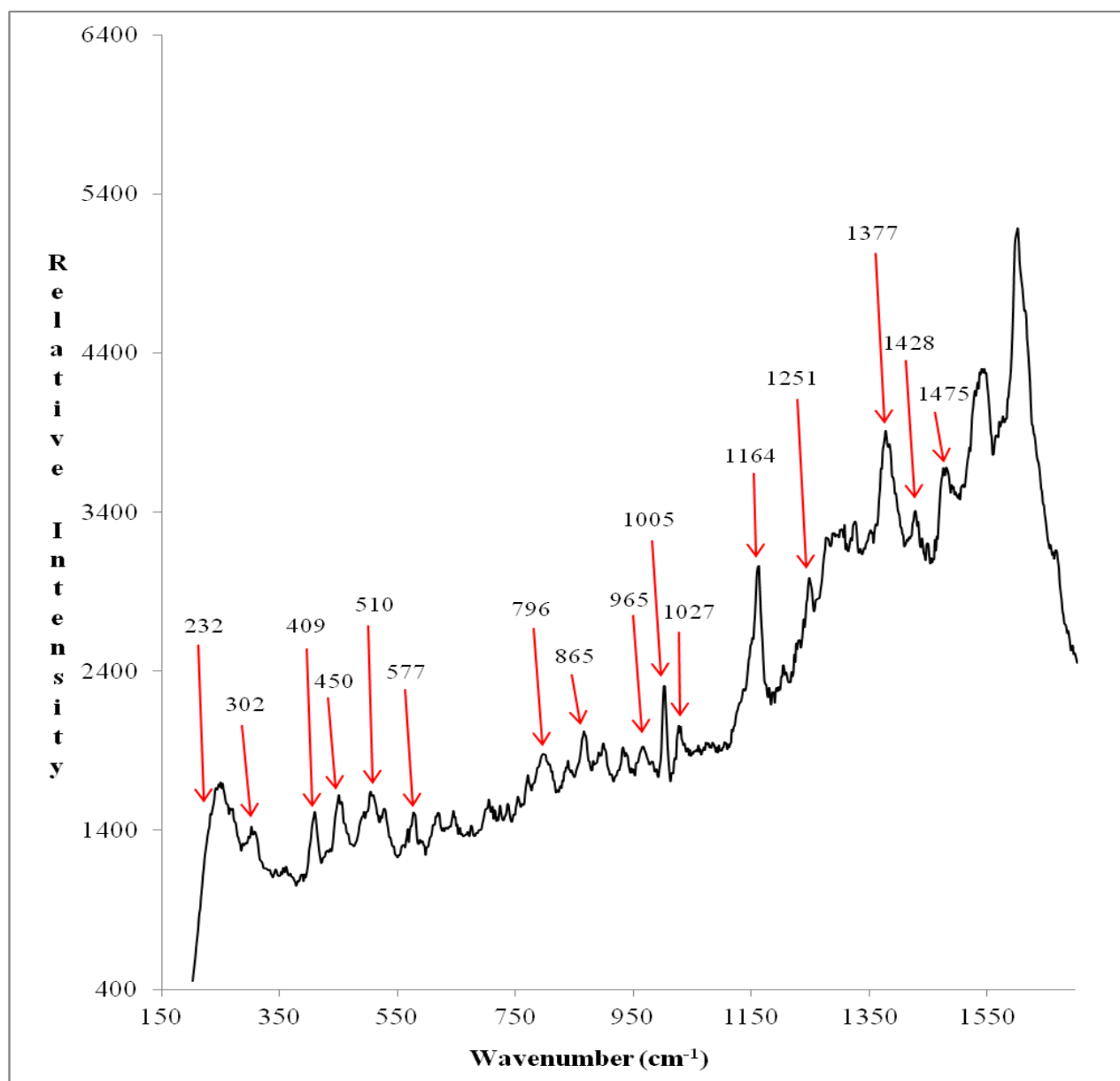


Figure 6. SERS results from the aptamer solution of 0.1 μM concentration. Wavenumber in cm<sup>-1</sup> is on the x axis, and relative intensity on the y axis.

Table 1. Detailed results of aptamer solution of 0.1  $\mu$ M concentration.

SERS Experimental Wavenumber	SERS Literature Wavenumber	Raman Wavenumber	Assignment
232	230		Ag-Cl in Thymine
302	314		C <sub>2</sub> N <sub>1</sub> -C <sub>6</sub> N <sub>1</sub> Ring Bending in Thymine
450	470		C <sub>2</sub> N <sub>1</sub> C <sub>6</sub> bending and N <sub>3</sub> C <sub>4</sub> C <sub>5</sub> bending in cytosine and thymine
510	512	498	C <sub>2</sub> N <sub>1</sub> C <sub>6</sub> bending and N <sub>9</sub> Ring Bending C <sub>5</sub> C <sub>4</sub> N bending in guanine
577	586	565	N <sub>1</sub> C <sub>2</sub> N <sub>3</sub> bending and C <sub>2</sub> N <sub>3</sub> C <sub>4</sub> bending in Thymine
796	796	787	Ring breathing in cytosine
865	852	854	-N <sub>7</sub> C <sub>5</sub> stretching and N <sub>1</sub> C <sub>2</sub> N <sub>3</sub> bending in Guanine
965	960		N <sub>9</sub> Ring stretching and N <sub>3</sub> C <sub>2</sub> stretching in Guanine
1005	1020		NH <sub>2</sub> rocking and C <sub>6</sub> H bending in cytosine
1027	1028		NH <sub>2</sub> rocking and N <sub>9</sub> ring stretching in adenine
1164	1154		-C <sub>8</sub> N <sub>7</sub> stretching and N <sub>9</sub> Ring stretching and C <sub>4</sub> N <sub>3</sub> stretching in guanine
1251	1264	1254	N <sub>1</sub> C <sub>2</sub> stretching and C <sub>2</sub> H bending and N <sub>9</sub> C <sub>8</sub> stretching and C <sub>8</sub> N <sub>7</sub> stretching in Adenine
1377	1370	1362	C <sub>8</sub> N <sub>9</sub> stretching and C <sub>2</sub> N <sub>3</sub> stretching in Adenine

1428	1442	1456	C <sub>5</sub> -Me bending in Thymine
1475	1472		N <sub>1</sub> C <sub>2</sub> stretching and C <sub>2</sub> N <sub>3</sub> stretching

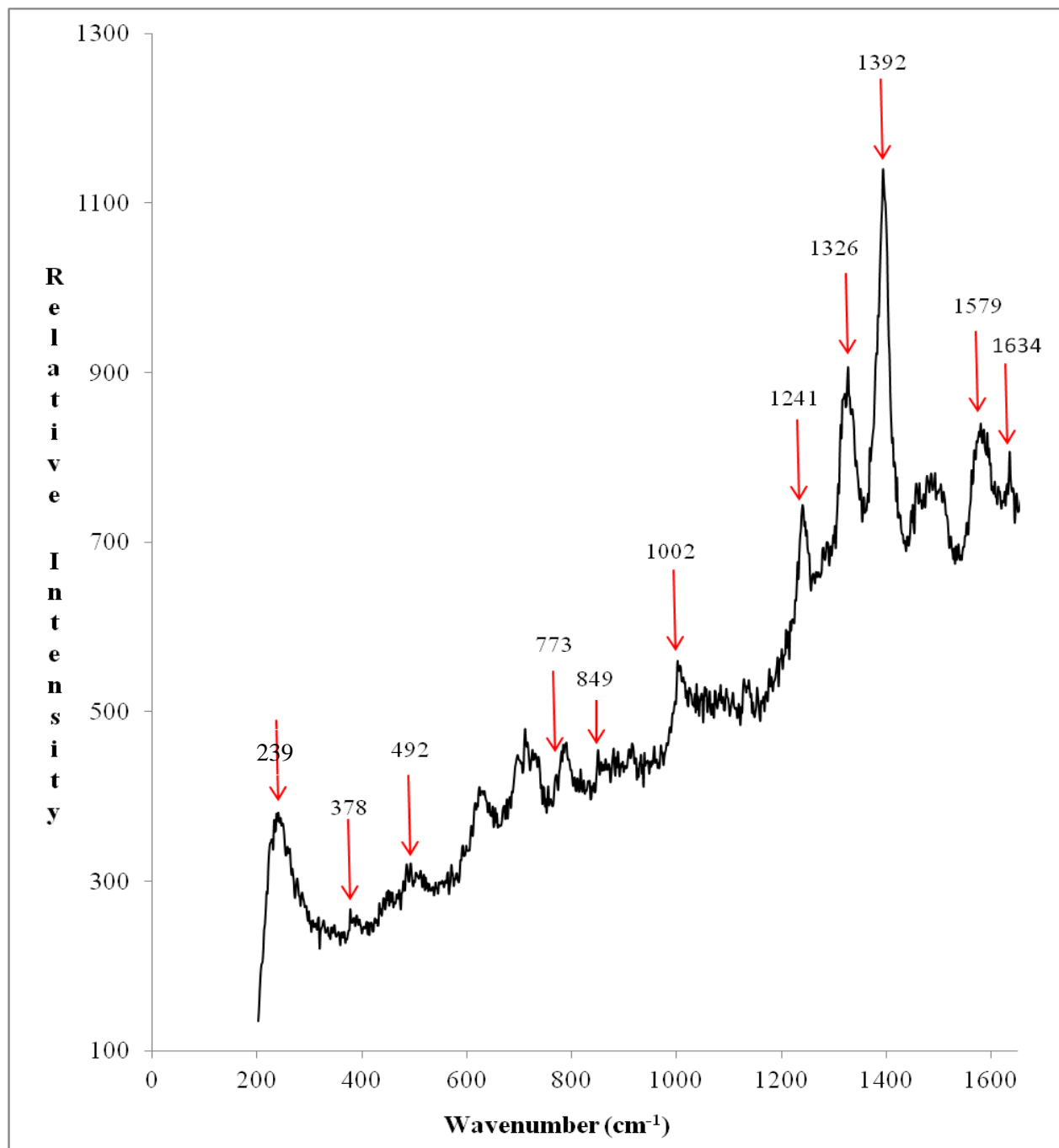


Figure 7. SERS results from the aptamer solution of 1.0  $\mu\text{M}$  concentration. Wavenumber in  $\text{cm}^{-1}$  is on the x axis, and relative intensity on the y axis.

Table 2. Detailed results of aptamer solution of 1.0  $\mu\text{M}$  concentration.

SERS Experimental Wavenumber	SERS Literature Wavenumber	Raman Wavenumber	Assignment
239	230		Ag-Cl in Thymine
378	370	382	$\text{C}_2\text{N}_{14}$ bending and $\text{N}_9$ Ring Bending in guanine
492	490	470	$\text{C}_2\text{N}_1\text{C}_6$ bending and $\text{N}_3\text{C}_4\text{C}_5$ bending in cytosine and thymine
773	776	750	Ring breathing in Thymine
849	852	854	$-\text{N}_7\text{C}_5$ stretching and $\text{N}_1\text{C}_2\text{N}_3$ bending in Guanine
1002	1020		$\text{NH}_2$ rocking and $\text{C}_6\text{H}$ bending in cytosine
1241	1222	1214	$-\text{C}_6\text{H}$ bending and $\text{C}_8\text{N}_7$ stretching in guanine
1326	1332	1364	$\text{C}_8\text{N}_9$ stretching and $\text{N}_7\text{C}_8$ stretching in guanine
1392	1390	1398	$\text{N}_1\text{C}_6$ stretching and $\text{C}_6\text{N}_{12}$ stretching in adenine
1579	1582	1576	$\text{N}_3\text{C}_4$ stretching and $\text{C}_4\text{C}_5$ stretching in Guanine
1579	1582		$\text{C}_4\text{C}_5$ stretching and $\text{C}_5\text{C}_6$ stretching in cytosine
1579	1582		$\text{N}_3\text{C}_4$ and $\text{N}_1\text{C}_2$ stretching and $\text{C}_5\text{C}_6$ stretching and $\text{N}_1\text{C}_6$ stretching in Thymine
1634	1640	1655	$\text{C}_2=\text{O}$ stretching and $\text{C}_2\text{N}_3$ stretching in cytosine

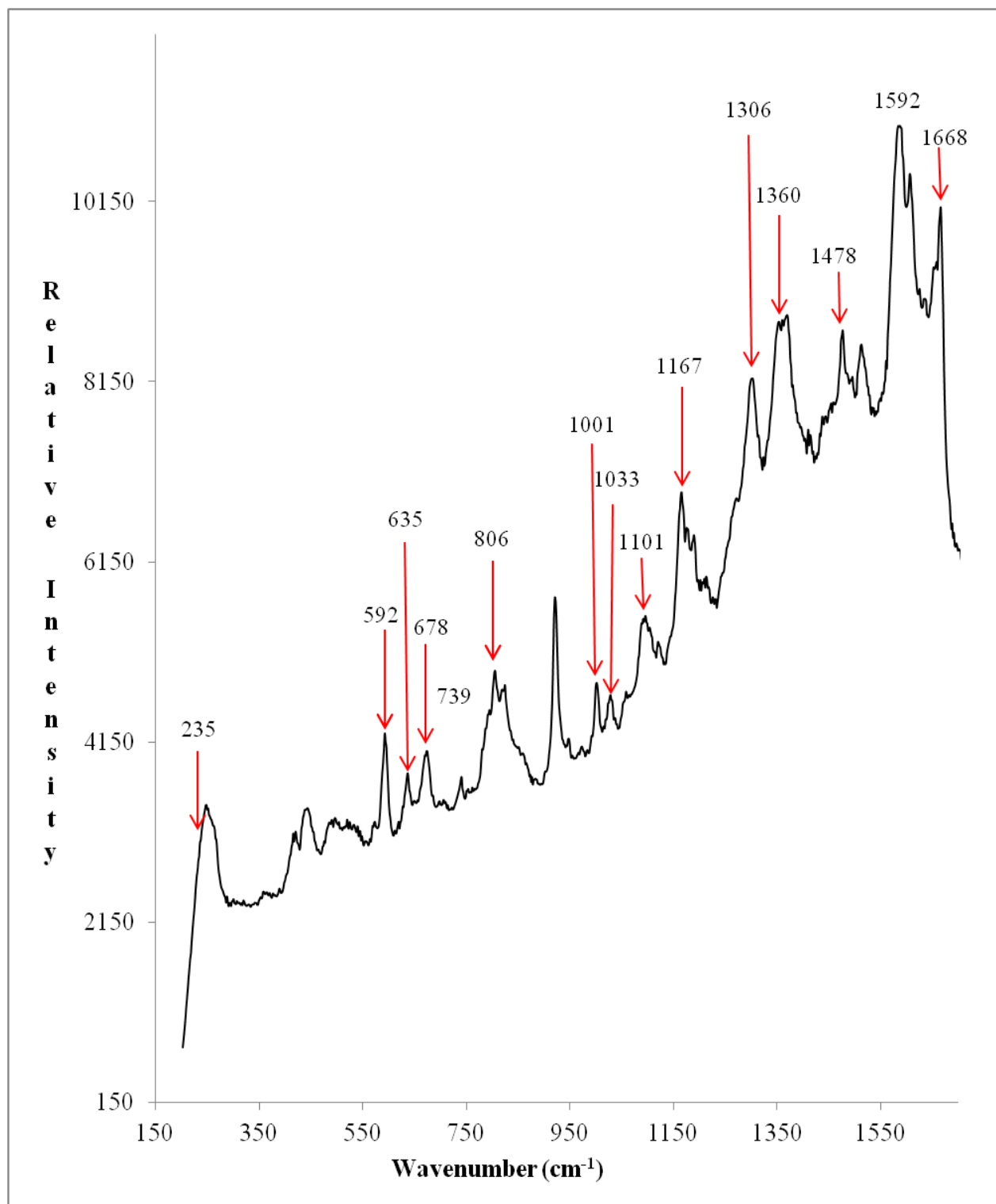


Figure 8. SERS results from from the aptamer solution of 2.0  $\mu\text{M}$  concentration. Wavenumber in  $\text{cm}^{-1}$  is on the x axis, and relative intensity on the y axis.

Table 3. Detailed results of aptamer solution of 2.0  $\mu\text{M}$  concentration.

SERS Experimental Wavenumber	SERS Literature Wavenumber	Raman Wavenumber	Assignment
232	230		Ag-Cl in Thymine
592	586	565	$\text{N}_1\text{C}_2\text{N}_3$ bending and $\text{C}_2\text{N}_3\text{C}_4$ bending in Thymine
635	632		$\text{N}_1\text{C}_2\text{O}$ bending and $\text{N}_3\text{C}_4\text{O}$ bending in thymine
678	690	498	$\text{C}_5\text{C}_4$ bending and $\text{N}_3\text{C}_4$ bending and $\text{N}_1\text{C}_2\text{O}$ bending $\text{N}_3\text{C}_2\text{O}$ bending in cytosine
739	732	724	Ring Stretching in adenine
806	796	787	Ring breathing in cytosine
1001	1020		$\text{NH}_2$ rocking and $\text{C}_6\text{H}$ bending in cytosine
1033	1028		$\text{NH}_2$ Rocking and $\text{N}_9$ Ring stretching
1101	1122	1124	$\text{N}_3\text{C}_2$ stretching and $\text{N}_9$ Ring stretching in adenine
1167	1154		$-\text{C}_8\text{N}_7$ stretching and $\text{N}_9$ Ring stretching and $\text{C}_4\text{N}_3$ stretching in guanine
1306	1306	1294	$\text{N}_1\text{C}_6$ stretching and $\text{C}_5\text{C}_6$ stretching in Cytosine
1360	1360	1368	$\text{C}_4\text{N}$ stretching and $\text{C}_5\text{C}_6$ stretching in Cytosine
1377	1370	1362	$\text{C}_8\text{N}_9$ stretching and $\text{C}_2\text{N}_3$ stretching in Adenine
1478	1472		$\text{N}_1\text{C}_2$ stretching and $\text{C}_2\text{N}_3$ stretching

1592	1582	1576	$N_3C_4$ stretching and $C_4C_5$ stretching in Guanine
1592	1582		$C_4C_5$ stretching and $C_5C_6$ stretching in cytosine
1592	1582		$N_3C_4$ and $N_1C_2$ stretching and $C_5C_6$ stretching and $N_1C_6$ stretching in Thymine
1668	1680	1680	$C_6=O$ stretching and $C_5C_6$ stretching in Guanine

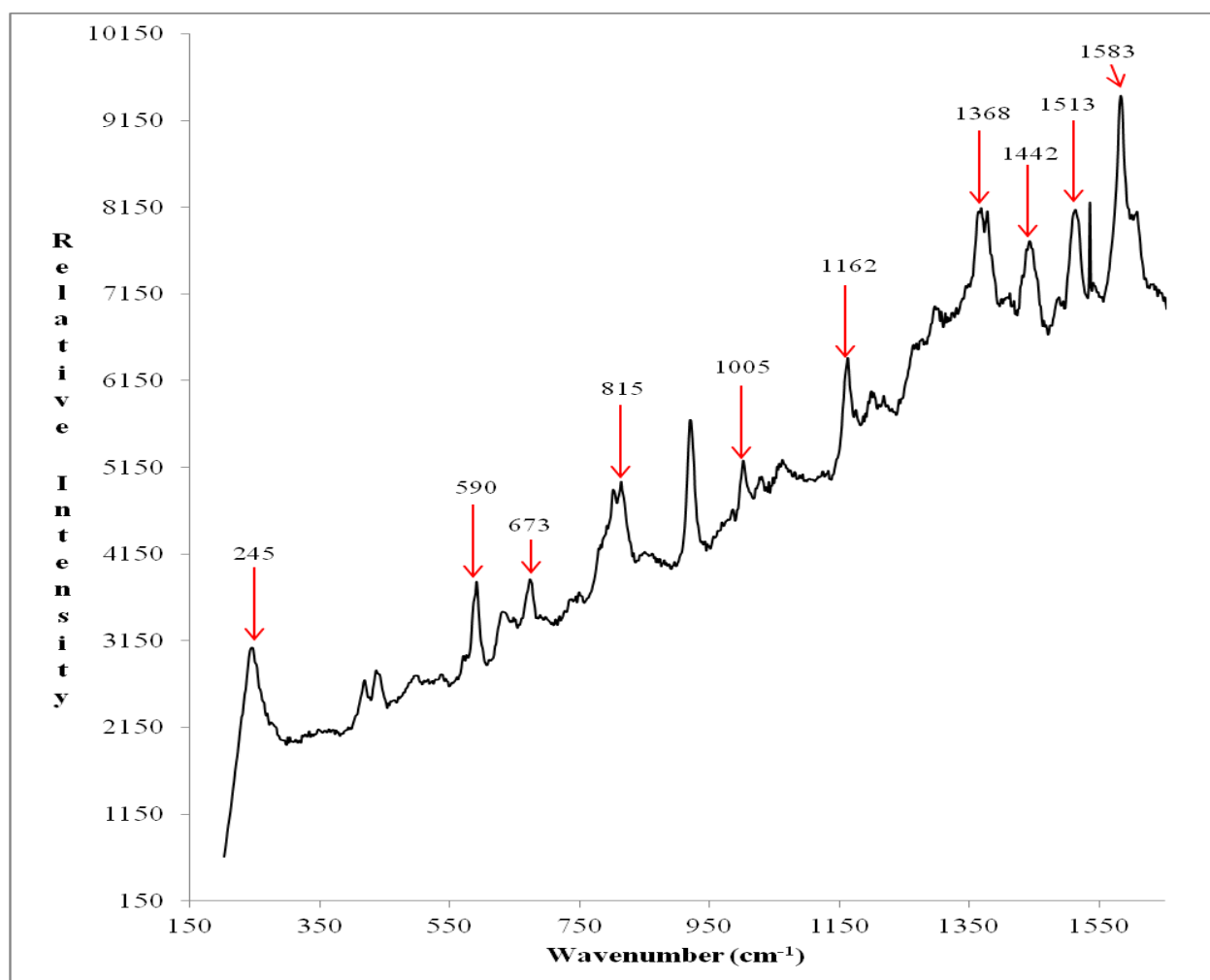


Figure 9. SERS results from from the aptamer solution of 5.0 μM concentration. Wavenumber in  $cm^{-1}$  is on the x axis, and relative intensity on the y axis.

Table 4. Detailed results of aptamer solution of 5.0  $\mu\text{M}$  concentration.

SERS Experimental Wavenumber	SERS Literature Wavenumber	Raman Wavenumber	Assignment
245	230		Ag-Cl in Thymine
590	586	565	$\text{N}_1\text{C}_2\text{N}_3$ bending and $\text{C}_2\text{N}_3\text{C}_4$ bending in Thymine
673	690	498	$\text{C}_5\text{C}_4$ bending and $\text{N}_3\text{C}_4$ bending and $\text{N}_1\text{C}_2\text{O}$ bending $\text{N}_3\text{C}_2\text{O}$ bending in cytosine
739	732	724	Ring Stretching in adenine
815	796	787	Ring breathing in cytosine
1005	1020		$\text{NH}_2$ rocking and $\text{C}_6\text{H}$ bending in cytosine
1162	1154		$-\text{C}_8\text{N}_7$ stretching and $\text{N}_9$ Ring stretching and $\text{C}_4\text{N}_3$ stretching in guanine
1368	1360	1368	$\text{C}_4\text{N}$ stretching and $\text{C}_5\text{C}_6$ stretching in Cytosine
1442	1442	1456	$\text{C}_5\text{Me}$ bending in Thymine
1513	1504	1503	N-H bending in thymine
1583	1582		$\text{C}_4\text{C}_5$ stretching and $\text{C}_5\text{C}_6$ stretching in cytosine
1583	1582		$\text{N}_3\text{C}_4$ and $\text{N}_1\text{C}_2$ stretching and $\text{C}_5\text{C}_6$ stretching and $\text{N}_1\text{C}_6$ stretching in Thymine
1583	1582		$\text{N}_3\text{C}_4$ and $\text{N}_1\text{C}_2$ stretching and $\text{C}_5\text{C}_6$ stretching and $\text{N}_1\text{C}_6$ stretching in Thymine

#### **4.5. Discussion and Conclusion**

The purpose of doing Surface Enhanced Raman Spectroscopy on the aptamer for IgE was to obtain a molecular fingerprint for the aptamer. Many previously identified peaks for the nucleic acid bases were seen in the experimental data. However, there was no correlation or pattern observed. However, the most peaks seem to appear in the 2.0  $\mu\text{M}$  solution. In future studies, in order to obtain a consistent molecular fingerprint, solutions in the range of concentrations from 0.1  $\mu\text{M}$  to 2.0  $\mu\text{M}$  can be used in order to see which concentration has the most peaks. Also, the laser transmission can be changed in order to see which transmission has the most peaks. Based on the aptamer found in the literature to be specific for the antibody Immunoglobulin E, a quantum-dot based aptamer beacon was designed for the detection of Immunoglobulin E. The results of these studies have been reported and presented via poster presentation in Phonons 2012 conference, and in a joint review paper about DNA and RNA aptamer nanosensors (Ranginwala)(Sen Et al).

#### **CITED LITERATURE**

1. Keefe, A.D., Pai, S., and Ellington, A. : Aptamers as therapeutics. Nature Reviews Drug Discovery. 9:537-550, 2010.
2. Xiao, Y., Lubin, A.A., Heeger, A.J., and Plaxco, K.W. Label-Free Electronic Detection of Thrombin in Blood Serum by Using an Aptamer-Based Sensor. Angew.Chem.Int.Ed. 44:5456-5459. 2005.
3. O'Donoghue, M.B., Shi, X., Fang, X., Tan, W., Single-molecule atomic force microscopy on live cells compares aptamer and antibody rupture forces. Anal Bioanal Chem. 402: 3205-3209. (2012).
4. Gupta, S., Thirstrup, D., Jarvis, T., Schneider, D., Wilcox, S., Carter, J., Zhang, C., Gelinas, A., Weiss, A., Janjic, N., Baird, G. Rapid Histochemistry Using Slow Off-rate Modified Aptamers With Anionic Competition. Appl Immunohistochem Mol Morphol 19: 273-278. 2011.

5. Dua, P., Kim, S., Lee, D. Patents on SELEX and Therapeutic Aptamers. Recent Patents on DNA & Gene Sequences. 2:172-186. 2008.
6. Iliuk, A.B, Hu, L., Tao, W.A. Aptamer in Bioanalytical Applications. Analytical Chemistry. 83: 4440-4452. 2011.
7. Owen, C. E. Immunoglobulin E: Role in asthma and allergic disease: Lessons from the clinic. Pharmacology and Therapeutics. 113:121-133. 2006.
8. Jamieson, T., Bakhshi, R., Petrova, D., Pocock, R., Imani, M., Seifalian, A.M. Biological applications of quantum dots. Biomaterials. 28: 4717-4732. 2007.
9. Held, Paul. Labautopedia The SLAS Knowledge Network. 20 June 2000. 22 August 2012 <[http://www.labautopedia.com/mw/index.php/An\\_Introduction\\_to\\_Fluorescence\\_Resonance\\_Energy\\_Transfer\\_\(FRET\)\\_Technology\\_and\\_its\\_Application\\_in\\_Bioscience](http://www.labautopedia.com/mw/index.php/An_Introduction_to_Fluorescence_Resonance_Energy_Transfer_(FRET)_Technology_and_its_Application_in_Bioscience)>.
10. Le Reste, L., Hohlbein, J., Gryte, K., Kapanidis, A.N. Characterization of Dark Quencher Chromophores as Nonfluorescent Acceptors for Single-Molecule FRET. Biophysical Journal. 102:2658-2668. 2012.
11. Wu, Z., Zheng, F., Shen, G., Yu, R. A hairpin aptamer-based electrochemical biosensing platform for the sensitive detection of proteins. Biomaterials 30: 2950-2955. 2009.
12. Science Technologies. Essential Biochemistry. 2004. 12 April 2012 <[http://www.wiley.com/college/pratt/0471393878/student/review/thermodynamics/4\\_gibbs.html](http://www.wiley.com/college/pratt/0471393878/student/review/thermodynamics/4_gibbs.html)>.
13. Zuker, M. Mfold web server for nucleic acid folding and hybridization prediction. Nucleic Acids Res. 31: 3406-3415. 2003.
14. Das, R.S., Agrawal, Y.K. Raman spectroscopy: Recent advancements, techniques and applications. Vibrational Spectroscopy. 57:163-176. 2011.
15. Otto, C., van den Tweel, T.J.J., de Mul, F. F. M., Greve, J. Surface-Enhanced Raman Spectroscopy of DNA Bases. Journal of Raman Spectroscopy. 17:289-298. 1986.

16. Tu, Q., Chang C. Diagnostic applications of Raman spectroscopy. Nanomedicine: Nanotechnology, Biology, and Medicine. 8:545-558.2012.
17. Abell, J.L., Driskell, J.D., Dluhy, R.A., Tripp, R.A., Zhao, Y.P. Fabrication and characterization of a multiwell array SERS chip with. Biosensors and Bioelectronics 24: 3663-3670. 2009.

#### **4.7. BIBLIOGRAPHY**

Saadia Ranginwala, Kimber Brenneman, Xenia Meshik, Justin Abell, Yiping Zhao, Michael Stroschio, and Mitra Dutta, "Surface Enhanced Raman Spectroscopy of DNA Aptamer for Immunoglobulin E". PHONONS 2012, July 8-12, 2012, Ann Arbor, Michigan.

B. Banani Sen, Shipryia Poduri, Ke Xu, Xenia Meshik, Saddia M. Ranginwala, Pitamber Shukla, and Nanzhu Zhang. "Nanosensors based on DNA and RNA Aptamers, and Semiconductor Quantum Dots." *CRC Dekker Encyclopedia on Nanoscience and Nanotechnology*. in press, 2012.

**VITA**

<b>Name:</b>	Saadia Ranginwala
<b>Education:</b>	B.S., Biochemistry, Minnesota State University, Mankato, MN, 2008 M.S., Bioengineering, University of Illinois at Chicago, Chicago, IL, 2012
<b>Research:</b>	Research project with Dr. Michael Stroschio, 2011-2012 working with aptamers and Raman Spectroscopy, only Substrate Enhanced Raman Spectroscopy